Spatial Neighborhood Mutual Information based Satellite Image Change Detection

Neha Gupta, and Samit Ari
Department of Electronics and Communication Engineering,
National Institute of Technology, Rourkela, India 769008.
Email: neha27brs@gmail.com, samit@nitrkl.ac.in

Abstract—Change detection deals with the problem of detecting changes that have occurred between various multi-temporal satellite images. This issue can be accomplished by measuring the similarity among these images. Therefore, in this paper, a very simple and effective change detection technique based on mutual information (MI), which is used as a similarity measure tool between two variables in statistics, is proposed. Herein, spatial neighborhood information around each pixel is exploited to get the MI and corresponding features. Further, difference feature vectors are created in feature space that provides discriminant information for change detection task. These difference feature vectors from all bands of multispectral images are concatenated to get the final feature vectors. Finally, features are classified by applying hard and soft clustering techniques i.e. k-means and fuzzy c-means, respectively and the results by both the clustering algorithms are compared. Experiments are conducted on two bitemporal satellite images, which confirm the effectiveness of the proposed technique.

Index Terms—Change detection, fuzzy c-means clustering, k-means clustering, Mutual information (MI).

I. INTRODUCTION

Remote sensing can be seen as the process of monitoring or collecting data about the earth's surface at places that are located far away. With the help of remote sensing, inaccessible or dangerous areas of the earth can be easily detected timely. Remote sensing images, which are the major source of remote sensing system, provide opportunity to scan large areas of the Earth's surface, as it allows us to observe much more than what we can do by standing on the ground. Some specific applications of the remote sensing images involves tracking of clouds to predict weather, changes on forests or farmland, mapping the ocean bottom, and large forest fires etc. A number of airborne and spaceborne sensors are available, which provide remote sensing images to observe far away areas promptly. Herein, the optical remote sensing images acquired by satellite are used to detect changes on the earth surface that have occurred within a time period [1].

Many unsupervised methods have been presented to perform change detection on earth's surface. Some of them consider the spatial neighborhood information, whereas some of them perform change analysis without spatial neighborhood information taking into account. Moreover, it has been seen that few change detection methods introduced feature level difference image to provide better results. In [2], local spatial contextual features are extracted by applying Gabor wavelet transform on log-ratio image, and two-level clustering is performed to get the binary change map. Binary descriptors are applied on individual images [3], and then Lloyd−Max's algorithm is applied on the Hamming distance that is obtained in the feature space. In [4]–[6], binary descriptor based technique is again applied on local patch by using inter image information. Furthermore, in [7], difference features are extracted in feature space or kernel transformed space that provide better results. In [8], two different kinds of difference images are generated by using subtraction and log ratio operator, which are integrated after applying mean and median filter, respectively. After that, the integrated difference image is partitioned into two classes by using k-means (KM) clustering algorithm. Such a combination of difference image provides the advantage of local consistency and smoothness obtained by the mean filter and preservation of edge information obtained by the median filter. In addition, Erreur Relative Globale Adimensionnelle de Synthese (ERGAS) index is applied in the local neighborhood to generate the gray scale image instead of directly applying on two images [9]. As mentioned in [10], preclassification of pixels is performed based on Gabor feature and hierarchical fuzzy c-means (FCM) algorithm in the first stage. Then, the second stage considers the patches corresponding to interested pixels position that are trained with PCANet Model. Finally, in the third stage, results of preclassification and PCANet stages are combined to get the binary change map. This trained PCANet model, which uses representative neighborhood pixels, provides robustness to speckle noise. Additionally, on the basis of the input-space textures, the output-space label-neighborhood information are extracted to construct the lable-information (LI) kernel [11]. Incorporation of spatial-contextual information using an anisotropic texture analysis, label-information composite (LIC) kernel provides strong noise immunity and accurate edge locations of the changed regions. However, without considering spatial neighborhood information, automatic thresholding by Expectation maximization (EM) technique provide more false alarms in [12].

As mentioned above, incorporating local neighborhood information, and generating difference data in feature space, both strategies provide better performance in change detection analysis of remote sensing images. Motivated by this, this work proposes a spatial neighborhood mutual information (MI) based technique, where MI is calculated between the spatial neighborhood information of both the satellite images for each pixel position and the difference data is generated in the feature space. MI provides the amount of information shared by one variable about another. Also, It has been used in the field of remote sensing as multimutual information (M-MI)

and multicontextual mutual information data (MMID) for post-earthquake building damage assessment and SAR image analysis, respectively. Here, MI based features are generated for single band, and then, features from all bands are concatenated to utilize the information coming from all bands. Once the final features are obtained, binary change map is created by using hard and soft clustering separately and the results with these clustering algorithms are compared. FCM and KM clustering algorithms are used as soft and hard clustering in this work, respectively [13], [14]. The proposed method according to two clustering algorithms are named as spatial neighborhood mutual information k-means (SNMIKM) and spatial neighborhood mutual information fuzzy c-means (SNMIFCM), respectively.
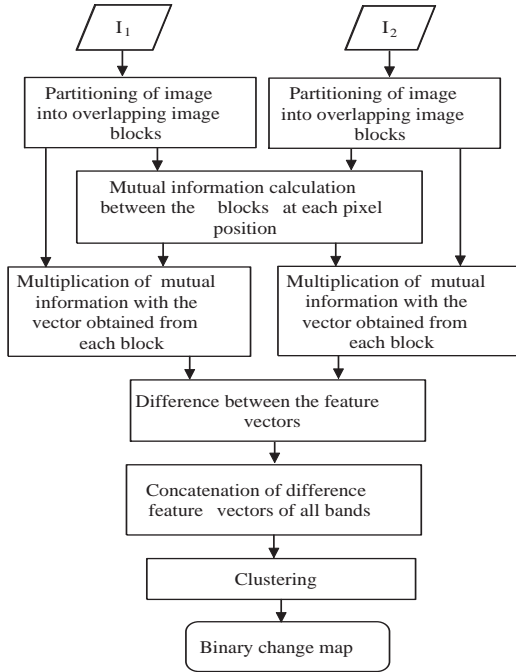

Fig. 1. Block diagram of the proposed technique.

II. PROPOSED METHODOLOGY

The purpose of this technique is to generate the change map, which contains the change and no change pixels. To achieve this goal, we consider two multispectral coregistered bitemporal satellite images of the same geographical location over a certain period of time. Suppose I_1 and I_2 are the single-channel satellite images with size of $L_1 \times L_2$ pixels. Mutual information, which is based on joint entropy, is used as a similarity measure tool in the proposed change detection framework to identify the changes between two multidate satellite images. Fig. 1 shows the block diagram of the proposed method, which consists of the following steps: multidate images partitioning; calculation of spatial neighborhood MI; generation of difference feature vector; binary map generation. The detailed description of the proposed method is given below.

A. Partitioning of both multi-date satellite images

In first step, multi-date images I_1 and I_2 are partitioned into $l \times l$ overlapping patches or blocks. Hence, there will

be two patches from two images for each pixel, and the center pixel of each patch is the the interested pixel. These patches are represented as P_1 and P_2 for further analysis.

B. Calculation of MI

As mentioned above, corresponding to each pixel position, there are two patches, which are obtained from both the satellite images. These patches are utilized to compute the MI for each pixel position. Therefore, it is considered as spatial neighborhood MI in this work.

MI can be seen as a concept that measure the amount of information contained by one variable about another. MI has an advantage that it doesn't require any prior relationship between two variables or images. In addition, as a similarity measure, MI analysis is based on the statistical relationship of variables or images joint entropy. MI is calculated by considering both individual entropies and joint entropy of both the variables. It is defined as follows:

$$MI(P_1, P_2) = H(P_1) + H(P_2) - H(P_1, P_2) \quad (1)$$

where $H(P_1)$ and $H(P_2)$ are the entropies of the patch of I_1 and I_2 images respectively, $H(P_1, P_2)$ denote the joint entropy and these entropies are defined as follows:

$$H(P_1) = -\sum p_1(r) \log_2 p_1(r) \quad (2)$$

$$H(P_2) = -\sum p_2(s) \log_2 p_2(s) \quad (3)$$

$$H(P_1, P_2) = -\sum p_{12}(rs) \log_2 p_{12}(r, s) \quad (4)$$

where r and s represent the pixel location in the patch P_1 and P_2 of I_1 and I_2 images respectively. $p_{12}(r, s)$ is the probability of a pair of the joint pixels r and s of the patch P_1 and P_2, respectively.

C. Creation of feature vectors

In this step, feature vectors for both the satellite images are created by using the spatial neighborhood MI, which is computed for each pixel position. To create the feature vectors, each patch of of both I_1 and I_2 images is converted into the vector. After that, spatial neighborhood MI of each pixel position are multiplied with the vectors, which are created by the patch of each image. The vectors corresponding to each patch of multi-date images are represented as

$$V_1(b_1, b_2) = \{x_1, x_2, \cdots, x_R\} \quad (5)$$

$$V_2(b_1, b_2) = \{y_1, y_2, \cdots, y_R\} \quad (6)$$

where R denotes the number of pixels available in patch of I_1 and I_2 image, (b_1, b_2) is the pixel position in image where $b_1 = \{1, 2, \cdots, L_1\}$ and $b_2 = \{1, 2, \cdots, L_2\}$.

Now feature vectors corresponding to each pixel position for both the I_1 and I_2 images are calculated as follows:

$$F_{v1}(b_1, b_2) = MI_{b_1, b_2}(P_1, P_2) \times V_1(b_1, b_2) \quad (7)$$

$$F_{v2}(b_1, b_2) = MI_{b_1, b_2}(P_1, P_2) \times V_2(b_1, b_2) \qquad (8)$$

where F_{v1} and F_{v2} are the feature vector of I_1 and I_2 images, respectively, at each pixel position.

D. Generation of difference feature vectors

Taking difference of features in transformed feature space always provides efficient features with respect to taking difference in original domain. Therefore, instead of directly working in difference image, here, difference is taken between the features extracted from both images. The difference feature vector is represented as follows:

$$D_{fv}(b_1, b_2) = F_{v1}(b_1, b_2) - F_{v2}(b_1, b_2). \qquad (9)$$

E. Concatenation of difference feature vectors

Since satellite images have multiple spectral bands, it is worthwhile to use all bands in change detection analysis, as it provides more information. Therefore, features from all the bands are combined to get the final feature vectors. Similarly as before, the difference feature vectors are created for all the bands. After that, these feature vectors are concatenated corresponding to each pixel position. The concatenated feature vectors are represented as follows:

$$\upsilon(b_1, b_2) = [D_{fv}^1(b_1, b_2), D_{fv}^2(b_1, b_2), \cdots, D_{fv}^B(b_1, b_2)] \qquad (10)$$

where B is the number of spectral bands. The final feature vectors of all pixels are represented as

$$\chi = [\upsilon_1, \upsilon_2, \cdots, \upsilon_{L_1 L_2}]^T. \qquad (11)$$

F. Clustering for generation of change detection map

As it is known that there is unavailability of training samples, therefore, classification of the feature vectors is accomplished by unsupervised clustering. Clustering can be described as assigning the set of objects into groups of similar objects and these groups can be called as clusters. There are two types of clustering algorithm exists as hard and soft clustering. Here, KM and FCM clustering is used as hard and soft clustering, respectively. The final features are classified by both clustering algorithms and performance of both clustering are compared. FCM is introduced as extended version of KM clustering algorithm. Both clustering techniques are described as follows.

1) KM clustering: KM clustering is designed to partition the observations into the defined number of clusters according to the nearest mean [14]. To find hard partitioning of all pixels, the KM algorithm is applied on χ by minimizing the following objective function

$$\mathcal{J}(\mathcal{V}) = \sum_{j=1}^{c} \sum_{k=1}^{S_j} (\|\upsilon_k - \nu_j\|)^2 \qquad (12)$$

$$\nu_j = (1/S_j) \sum_{j=1}^{S_j} \upsilon_k \qquad (13)$$

where $\mathcal{V} = [\nu_1, \nu_2]$ denotes the cluster's centroids. c represents the number of cluster centers. S_i is the number of observation points in ith cluster.

The labels in KM clustering is obtained by iteratively minimizing the sum of distances from each observation to its cluster centroid. The observations are moved within clusters until the sum in objective function cannot be decreased further.

2) FCM clustering: FCM is a soft clustering algorithm in which every data point may belong to more than one cluster rather than belonging to just one cluster as in KM clustering. Here, data is partitioned by assigning the membership grades to each observation, which belongs to each of the cluster instead of belonging to only one cluster as in hard clustering [13]. To find fuzzy partitioning of all pixels, the FCM algorithm is applied on χ by minimizing the objective function

$$\mathcal{J}_d(\mathcal{U}, \mathcal{V}) = \sum_{j=1}^{c} \sum_{k=1}^{L_1 L_2} \mu_{jk}^d \|z_k - \nu_j\|^2 \qquad (14)$$

$$\text{s.t.} \quad \mu_{jk} \in [0, 1], \sum_{j=1}^{c} \mu_{jk} = 1 \quad \forall k, \qquad (15)$$

$$0 < \sum_{k=1}^{L_1 L_2} \mu_{jk} < L_1 L_2 \quad \forall j \qquad (16)$$

where d is the degree of fuzziness and it is taken as $d \in [1, +\infty)$. μ_{jk} is the membership grade that belongs to ith cluster for jth pixel and represented with the partition matrix $\mathcal{U} = [\mu_{jk}]_{c \times L_1 L_2}$.

Fuzzy partitioning is performed by updating the membership grade μ_{jk} and the cluster centroids ν through an iterative optimization of the objective function $\mathcal{J}_d$. Here, $d = 2$, number of clusters, $c = 2$ are taken, and the iteration procedure is initialized at $l = 0$.

The centroids and membership grades are calculated as follows:

$$\nu_j^{(l+1)} = \frac{\sum_{k=1}^{L_1 L_2} \left(\mu_{jk}^{(l)}\right)^d z_k}{\sum_{k=1}^{L_1 L_2} \left(\mu_{jk}^{(l)}\right)^d} \qquad (17)$$

$$\mu_{jk}^{(l+1)} = \frac{\left\| z_k - \nu_j^{(l+1)} \right\|^{-2/(d-1)}}{\sum_{r=1}^{c} \mu_{jk}^d \left\| z_k - \nu_r^{(l+1)} \right\|^{-2/(d-1)}}. \qquad (18)$$

The above created feature vectors are clustered by the both clustering techniques, and the individual binary change map is generated on the basis of index value that are calculated by each clustering technique.

III. EXPERIMENTAL RESULTS

To get the effectiveness of the proposed method, the experiments are tested on two real data sets. These remote sensing images having multiple bands are acquired by different sensors of Landsat satellite.
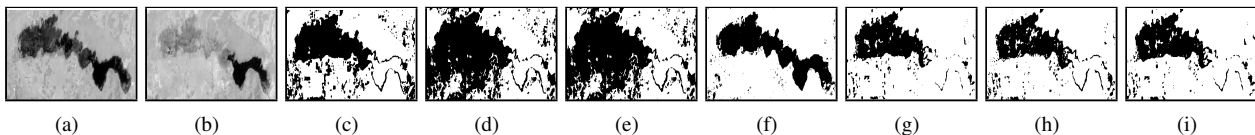
Fig. 2. Satellite image change detection results of dataset I. (a) and (b) Landsat-7 (NIR band) multitemporal images. (c) reference map or ground truth. (d) EM method. (e) BDLM method. (f) KKM method. (g) GaborTLC method. (h) and (i) SNMIKM and SNMIFCM method, respectively.
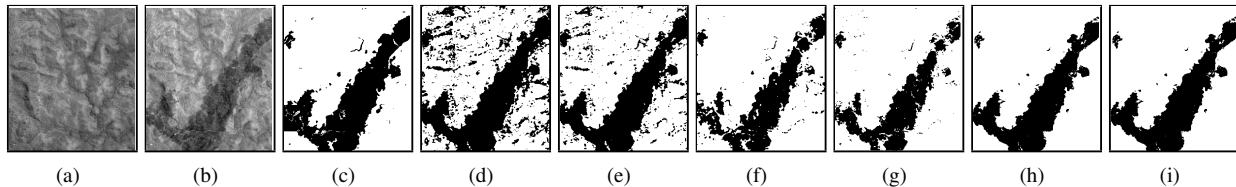

Fig. 3. Satellite image change detection results of dataset II. (a) and (b) Landsat-8 (NIR band) multitemporal images. (c) Reference map or ground truth. (d) EM method. (e) BDLM method. (f) KKM method. (g) GaborTLC method. (h) and (i) SNMIKM and SNMIFCM method, respectively.

A. Datasets Description

1) Dataset I: This pair of multitemporal images is captured by Landsat 7 Enhanced Thematic Mapper Plus (ETM+) sensor. The observing site is Natural Lake, Rajasthan, India. They are captured on February 09, 2001 and September 21, 2001 [6], [15], [16]. The size of the images is 220×550 pixels. The main land change is the dried lake due to summer.

2) Dataset II: This pair of multitemporal images is captured by Operational Land Imager (OLI) sensor of Landsat 8. The observing site is Yambulla State Forest, Australia. They are captured on October 01, 2015 and February 06, 2016 [15]. The size of the images is 320×260 pixels. Bushfire is the main land change that occurred across the Gold Mine road.

B. Qualitative Results

Basically, visual results are analyzed in qualitative assessment, which allows to decide the generated change map, roughly. The visual results of dataset I and II are shown in Fig. 2 and 3, respectively, where the appeared black and white pixels correspond to changed and unchanged region, respectively. Here, binary change maps are obtained by applying majority filter as a postprocessing operation [17]. Experimental results of the proposed method are compared with techniques like BDLM [3], EM [12], GaborTLC [2], and kernel k-means (KKM) [7] methods. By visualizing the qualitative results, it can be observed that EM and BDLM techniques produces noisy results due to detection of more false alarms. KKM and GaborTLC technique provide noise free results but still false alarms are more in KKM method than the proposed one. The information of unchanged and change pixels are detected better in the proposed method compared to the reported techniques. Small changes along with the major changed area are also detected with less false alarms in the proposed method because it considers the spatial neighborhood information around each pixel for feature extraction. Although better visual results are provided by proposed method, still it fails to detect some part of changed area. When there is less variation in values of changed pixels and all pixels present in any block or patch are changed pixels then the value of MI between them will be comparatively less. Hence, this variation will not be reflected in feature vectors obtained after multiplication

of MI and these pixels will be detected as unchanged even though they are changed.

Table I
PERFORMANCE MEASURES (%) FOR DATA SET I AND II

Datasets	Method	P_{CC}	P_{FA}	P_{TE}	κ
Dataset I (Natural Lake)	EM [12]	80.69	25.17	19.31	60.55
	BDLM [3]	80.80	25.00	19.20	60.74
	KKM [7]	80.85	8.36	19.15	53.21
	GaborTLC [2]	87.99	0.24	12.01	69.63
	SNMIKM	88.11	0.54	11.89	70.09
	SNMIFCM	88.40	0.32	11.60	70.79
Dataset II (Yambulla State Forest)	EM [12]	84.74	17.22	15.26	66.51
	BDLM [3]	89.96	8.43	10.04	76.52
	KKM [7]	91.50	1.40	8.50	78.48
	GaborTLC [2]	89.82	1.16	10.18	73.68
	SNMIKM	94.41	1.10	5.59	86.18
	SNMIFCM	94.52	1.10	5.48	86.46

C. Quantitative Results

Here, change map is compared with ground truth based on some predefined parameters [2], [3], which are characterize as follows: 1) Overall accuracy or correct classification or (OA) or (P_{CC}), 2) False positives or false alarms (P_{FP} or P_{FA}): the number of "unchanged" pixels which are detected as "changed", 3) Total error (P_{TE}), 4) Kappa coefficient (κ). To compare the proposed method with the EM [12], BDLM [3], KKM [7], and GaborTLC [2] methods, the reported techniques are implemented in the same way as in [2], [3], [7], [12]. The performance results in terms of all measures is shown in Table I.

In comparison to earlier reported techniques as stated in Table I, the proposed technique yields better performance in terms of all parameters. The increased accuracy and kappa value, and reduced false alarms show the effectiveness of utilizing the spatial neighborhood MI in the proposed technique.

Sometimes may be the difference between the values of changed pixels at any location is very less, however, MI calculated for that location should be less but it became moderate due to the influence of neighboring pixels. As a result, features have very less variation that accounts for the changed pixels to be detected as unchanged. Moreover, may be the unchanged pixels are present at any location, therefore, values of those pixels are obviously very close to each other. However, MI calculated for that location may again give moderate value due to the
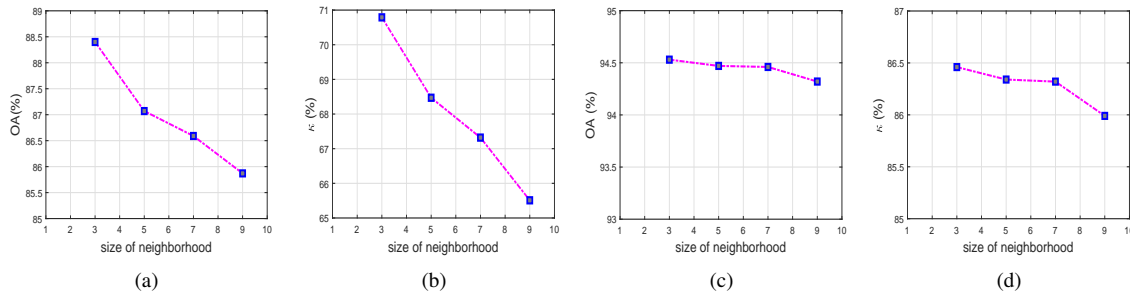
Fig. 4. The analysis of different patch sizes on the proposed method' performance. (a) and (b) OA and κ for dataset I. (c) and (d) OA and κ for dataset II.

influence of neighboring pixels. Consequently, features obtained after multiplication with MI have very less variation that accounts for the unchanged pixels to be overlapped with above mentioned changed pixels. Due to the above mentioned reasons, overlapping of features corresponding to unchanged and changed pixels is occurring. SNMIKM technique detects unchanged pixels very well but fails to detect changed one because of the presence of overlapping clusters. Therefore, SNMIFCM technique, which uses FCM clustering, performs better in overlapping clusters.

The performance of different patch sizes on all datasets for SNMIFCM method, which is better than the other proposed technique, is shown in Fig. 4. It is observed that kappa value and overall accuracy are decreasing as patch size is increasing for all datasets. It is analyzed that when patch size increases, more number of neighboring pixels are coming into account for feature vector generation. If the pixel at any location and majority of nearby pixels belong to different classes then that pixel is assigned to other class. Thus, changed and unchanged region are varying according to the effect of large patch size means surrounding pixels of actual changed areas are detected as changed due to large patch size. Similarly, surrounding pixels of actual unchanged areas are detected as unchanged due to large patch size.

IV. CONCLUSION

This paper proposes an unsupervised spatial neighborhood MI based technique. MI, which dose not require any prior relationship between variables being utilized, is calculated between the patches of both bitemporal satellite images. Feature vectors are created for each pixel position of multi-date images by considering the neighboring pixels around each pixel. This neighborhood information is multiplied with the MI to create feature vector space. Then, difference feature vectors, which are created in transformation space, provide more discriminant information for change detection task. Since the local neighborhood information is used in change analysis, this results in better performance. Two methodologies have been proposed where SNMIFCM provides better results compared to SNMIKM technique. Experiments performed on real multispectral satellite images demonstrate the capability of the proposed method.

ACKNOWLEDGMENT

REFERENCES

[1] A. Singh, "Review article digital change detection techniques using remotely-sensed data," *Int. J. Remote Sens.*, vol. 10, no. 6, pp. 989–1003, 1989.

[2] H.-C. Li, T. Celik, N. Longbotham, and W. J. Emery, "Gabor feature based unsupervised change detection of multitemporal SAR images based on two-level clustering," *IEEE Geosci. Remote Sens. Lett.*, vol. 12, no. 12, pp. 2458–2462, dec 2015.

[3] A. Radoi and M. Datcu, "Automatic change analysis in satellite images using binary descriptors and lloyd–max quantization," *IEEE Geosci. Remote Sens. Lett.*, vol. 12, no. 6, pp. 1223–1227, 2015.

[4] N. Gupta, G. V. Pillai, and S. Ari, "Unsupervised change detection in optical satellite images using binary descriptor," in *2017 International Conference on Wireless Communications, Signal Processing and Networking (WiSPNET)*. IEEE, mar 2017.

[5] G. V. Pillai, N. Gupta, and S. Ari, "Descriptors based unsupervised change detection in satellite images," in *2017 International Conference on Communication and Signal Processing (ICCSP)*. IEEE, apr 2017.

[6] N. Gupta, G. V. Pillai, and S. Ari, "Change detection in optical satellite images based on local binary similarity pattern technique," *IEEE Geosci. Remote Sens. Lett.*, vol. PP, no. 99, pp. 1–5, 2018.

[7] M. Volpi, D. Tuia, G. Camps-Valls, and M. Kanevski, "Unsupervised change detection with kernels," *IEEE Geosci. Remote Sens. Lett.*, vol. 9, no. 6, pp. 1026–1030, 2012.

[8] Y. Zheng, X. Zhang, B. Hou, and G. Liu, "Using combined difference image and k-means clustering for sar image change detection," *IEEE Geosci. Remote Sens. Lett.*, vol. 11, no. 3, pp. 691–695, 2014.

[9] D. Renza, E. Martinez, and A. Arquero, "A new approach to change detection in multispectral images by means of ergas index," *IEEE Geosci. Remote Sens. Lett.*, vol. 10, no. 1, pp. 76–80, 2013.

[10] F. Gao, J. Dong, B. Li, and Q. Xu, "Automatic change detection in synthetic aperture radar images based on pcanet," *IEEE Geosci. Remote Sens. Lett.*, vol. 13, no. 12, pp. 1792–1796, 2016.

[11] L. Jia, M. Li, Y. Wu, P. Zhang, G. Liu, H. Chen, and L. An, "Sar image change detection based on iterative label-information composite kernel supervised by anisotropic texture," *IEEE Trans. Geosci. Remote Sens.*, vol. 53, no. 7, pp. 3960–3973, 2015.

[12] L. Bruzzone and D. F. Prieto, "Automatic analysis of the difference image for unsupervised change detection," *IEEE Trans. Geosci. Remote Sens.*, vol. 38, no. 3, pp. 1171–1182, 2000.

[13] J. C. Bezdek, *Pattern recognition with fuzzy objective function algorithms*. Springer Science & Business Media, 2013.

[14] T. Kanungo, D. M. Mount, N. S. Netanyahu, C. D. Piatko, R. Silverman, and A. Y. Wu, "An efficient k-means clustering algorithm: Analysis and implementation," *IEEE Trans. Pattern Anal. Mach. Intell.*, vol. 24, no. 7, pp. 881–892, 2002.

[15] [Online]. Available: http://earthexplorer.usgs.gov/

[16] N. Gupta, G. V. Pillai, and S. Ari, "Change detection in landsat images based on local neighbourhood information," *IET Image Processing*, vol. 12, no. 11, pp. 2051–2058, nov 2018.

[17] X. Huang, Q. Lu, L. Zhang, and A. Plaza, "New postprocessing methods for remote sensing image classification: A systematic study," *IEEE Trans. Geosci. Remote Sens.*, vol. 52, no. 11, pp. 7140–7159, 2014.